Proceedings of the Canadian Society for Mechanical Engineering International Congress 2020
CSME Congress 2020
June 21-24, 2020, Charlottetown, PE, Canada

NUMERICAL SIMULATION OF LAMINAR VORTEX-SHEDDING FLOW AROUND A VERY SLENDER AND RECTANGULAR BLUFF BODY

Amin Etminan[1*], Armin Bodaghkhani[2], Yuri S. Muzychka[1]
[1]Department of Mechanical Engineering, Memorial University of Newfoundland (MUN), St. John's, NL, Canada
[2]Faculty of Sustainable Design Engineering, University of Prince Edward Island (UPEI), Charlottetown, PEI, Canada
*corresponding author's email: aetminan@mun.ca

Abstract—In the present study, the numerical results of flow and heat transfer structure around a very slender bluff body with a rectangular cross-sectional area are investigated in detail. The Reynolds number is considered so low that the flow presumably is laminar. Reynolds number, Prandtl number, aspect ratio, and the angle of incidence are assumed to be 100, 0.71, 0.1, and 45 degrees respectively. A finite volume method using the SIMPLEC algorithm and non-staggered grid is employed for the simulation in the two-dimensional and incompressible flow regime. The studies of spatial resolution and grid independency are carried out as well. Furthermore, the instantaneous variations of flow parameters are provided and discussed thoroughly. The global quantities including pressure and viscous drag and lift coefficients, the Root Mean Square (RMS) of drag and lift, and Strouhal number are also computed. The simulations reveal that the angle of incidence of the bluff body relocates the stagnation point from the centre to a point at the one-fifth of the frontal side. An acceptable verification has been observed by making a comparison between the provided results and available data in the literature.

Keywords- slender bluff body; SIMPLEC algorithm; unsteady flow; vortex shedding; heat transfer.

I. INTRODUCTION

The prediction and the analysis of flow characteristics over a slender bluff body have recently attracted significant attention in the field of aerodynamics and wind engineering. The essential and practical importance of an understanding of flow behavior around bluff bodies is still demanded by mechanical and aeronautical engineers. Despite the simple geometry of common bluff body objects such as square, circular, and rectangular, the flow analysis around them is very complicated. However, due to the complexity of the flow that usually comes across bluff bodies, the prediction of lift and drag forces, frequency of eddy shedding, and pressure distribution still disclose many curious facts for investigators. In recent decades, Computational Fluid Dynamics (CFD) has become one of the most popular and efficient method for the analysis of the flow structure in the early stage of each real construction and manufacturing process. Flow separation, vortex shedding, fluctuating lift and drag forces, vibration, noise, and heat transfer patterns around bluff bodies were extensively investigated by many researchers [1-8].

The effect of the orientation of a square cylinder on flow characteristics was experimentally studied by [9]. The angle of incidence was ranged from 0 to 60 degrees, and the Reynolds number was changed from 1340 to 9980. Their results disclosed that flow separation points were located at the leading edge of the cylinder with zero inclination. When the angle of orientation was greater than zero, the location of separation points was moved downstream, and the size of the wake region was increased. They also found that an increase in the angle of incidence caused a smaller drag coefficient and a higher Strouhal number. Particle Image Velocimetry (PIV) was used by [10] to capture the vortex shedding phenomenon caused by flow passing a two-dimensional square cylinder at incidence for Reynolds numbers of 4000, 10000, and 20000. A comprehensive study on the vortex shedding process and the coherent large-scale flow unsteadiness were done by [10] too.

The flow pattern around a square cylinder with two aspect ratios of 16 and 28, the angle of incidence varying between 0 and 45 degrees and a Reynolds number of 410 was investigated by [11]. PIV along with hot wire anemometry, were utilized to find flow parameters such as velocity, pressure, and fluctuations. The lowest drag coefficient and highest Strouhal number were found at 22.5° of incidence. The flow visualization images revealed that the streamwise space between the alternating vortices in the downstream was depended on the angle of incidence. They also observed that the drag coefficient was decreased and the Strouhal number was increased as the aspect ratio was enhanced.

Flow around a sharp-edged rectangular bluff body with an aspect ratio of 1:5 was studied by [12] using a high-pressure wind tunnel. By making a comparison between two angles of incidence (e.g., α=0 and 45 degrees), it was found that the distribution of the lift coefficient caused a reattachment for α=0° and consequently empowered the vortex shedding phenomenon.

The aerodynamic behavior of rectangular bluff body with an aspect ratio of 1:5 was investigated by [13 and 14] numerically and experimentally. In these comprehensive studies, all details of flow involving pressure distribution on the cylinder, drag and lift forces, as well as the vortex shedding phenomenon were investigated using a wind tunnel for unsteady high Reynolds number flow regime. They found that the size of the recirculation region near the lateral walls of the cylinder was decreased versus free-stream turbulence. They also showed that turbulence level affected the vortex shedding mechanism significantly and made the vibration of the flexible cylinder consequently. Wake measurement was done by a slight Reynolds number dependence of the Strouhal number frequency. Both numerical and experimental studies of flow structure around a rectangular bluff body with an aspect ratio of 5:1 was carried out by [15] using Large Eddy Simulation (LES). Two moderate and high turbulence inlets were considered as inlet boundary conditions. They found that shear layer instabilities appeared adjacent to the leading edge of the bluff body when the strong level of inlet turbulence flow was considered. Therefore, this instability made a higher shear layer curvature and a shorter reattachment length as well.

The main purpose of this numerical study is to investigate the incoming free-stream flow influence on aerodynamic forces applied on and heat transfer characteristics from a very slender bluff body with rectangular cross section area and sharp corners. Regarding the assumed Reynolds number, the flow regime is remained laminar. A comprehensive grid independency study is carried out to reveal optimal mesh size.

It is found that the vortex shedding phenomenon made by rectangular vortex generator can affect all fluid and thermal parameters throughout computational domains particularly downstream flow. The assumed boundary conditions and geometrical constants are presented in Fig. 1. Based on this figure, the dimensionless height of the domain is 20; upstream distance is 8.5 and downstream distance is 20. These constant values are suggested by several reputable studies such as [16-19]. The inlet X-velocity component of 1.0 is applied to the entrance while the fully developed boundary condition is employed at flow output as well. It means that the downstream distance is long enough that all flow parameters have no variation in X-direction. Moreover, two other sides of the domain are presumed far-field. It also indicates that these boundaries are not affected by the boundary layer created by the solid walls of the vortex generator. Eventually, no-slip boundary condition and constant wall temperature are considered on the heated bluff body, where placed at 45° of incidence (see Fig. 1).

II. Computational Method

The numerical analysis includes continuity, Navier-Stokes, energy, and other related equations for simulation of flow and heat transfer characteristics around the described bluff body. All simulations are conducted for a two-dimensional, incompressible, Newtonian and unsteady-periodic flow. The governing equations in dimensionless form are as follows:

$$U_{i,i} = 0 \tag{1}$$

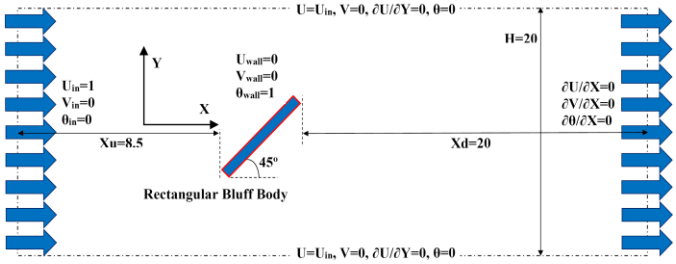

Figure 1. Geometrical details of the problem and coordinate system along with considered boundary conditions.

$$U_{i,\tau} + (U_i U_j)_{,j} = -P_{,i} + Re^{-1} U_{i,jj} \tag{2}$$

$$\theta_{,\tau} + (U_j \theta)_{,j} = (Re\ Pr)^{-1} \theta_{,jj} \tag{3}$$

where,

$X=x/d$, $Y=y/d$, $\tau=tu_{in}/d$, $P=p/(\rho u^2_{in})$, $U_i=u_i/u_{in}$ i.j=1, 2,

$\theta=(T-T_{in})/(T_w-T_{in})$

The Reynolds, Strouhal and Prandtl numbers are defined as follows:

$$Re = u_{in} d/\upsilon \tag{4}$$

$$St = fd/(u_{in}\upsilon) \tag{5}$$

$$Pr = \upsilon/\alpha \tag{6}$$

where d, f, t, T, ρ, ν, and α correspond to the projection of vortex generator height, the frequency of eddy shedding, time, temperature, density, kinematic viscosity, and thermal diffusion of fluid respectively. Furthermore, constant density, viscosity and dimensionless time-step of $\Delta\tau=0.025$ are considered to all simulations. The velocity-pressure coupling in the governing equations is based on the algorithm of the Semi-Implicit Method for Pressure Linked Equations-Consistent (SIMPLEC), and a second-order Crank–Nicolson scheme is utilized. The second-order upwind differencing scheme is applied for the spatial discretization of the pressure and momentum terms. To compute the global parameters such as aerodynamic forces, Strouhal number, drag and lift coefficients, and the RMS of these forces, a sampling time of 10 predominant vortex shedding cycles are considered.

III. Grid Generation

According to Fig. 1, the computational domain is a rectangle with a dimensionless size of 29.5×20. This area must be discretized to very small finite volumes for capturing all flow phenomena, particularly near the bluff body, where flow separation, reverse flow, pressure gradient, and shear flow are dominant matter. As illustrated in Fig. 2(a), quadrilateral meshes are generated entire the computational domain. With the first grid minimal setting 0.0005 away from the bluff body walls, the grids are stretched gradually with an expansion rate of 1.02 for 1×d dimension in both X- and Y-directions from the solid walls of the bluff body (see Fig. 2(b)).

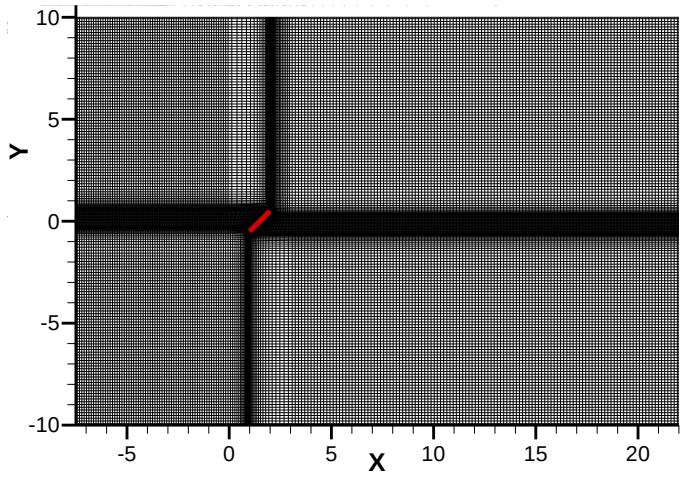

(a)

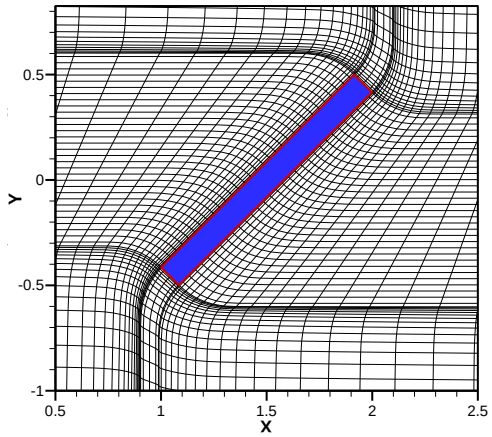

(b)

Figure 2. The schematic of generated grid (a) whole domain, (b) zoomed-in view of the area around the vortex generator.

IV. Numerical Approach Validation

In all numerical simulation methods, data validation is intended to make certain, well-defined, accurate, and precise numerical procedure as well as results. Table 1 shows some of the both numerical and experimental results in the literature. According to the data in Table 1, an acceptable agreement is observed between present study and others' results. Some differences between results are rooted in solution methods, different Reynolds number, and geometrical details.

V. Mesh Independency Study

A mesh independency study is carried out to find an optimal number of cells and the impact of the cell numbers on the flow parameters, i.e. mean drag coefficient and Strouhal number. Five non-uniform and structured cases of generated mesh including 24140, 32144, 38700, 46295 and 56680 volumes are provided to distinguish an independent grid number. Therefore, the variations of the drag coefficient and Strouhal number versus five mentioned grid cases are presented in Fig. 3. This figure clearly demonstrates a negligible deviation between the mentioned flow parameters for the grid number of 46295 and 56680. Consequently, grid number of 46295 should be selected to minimize the computational time for all simulations.

VI. Numerical Results and Discussion

Fig. 4 illustrates, where the time-histories of the lift and drag coefficients are drawn, the steady flow changes into an unsteady-periodic regime after a specific time, and these forces apply to the bluff body periodically with a constant frequency. It means that as the time-marching process is commenced, the time-histories experiences a transient start-up process reaching a fully saturated periodic flow. The period of the transient time depends on initial conditions, the Reynolds number, the aspect ratio, and the angle of incidence of the bluff body (as it mentioned by [16]), which is about τ=25 as it recognizable from Fig. 4. In this case the amplitude of drag force is 0.51 and

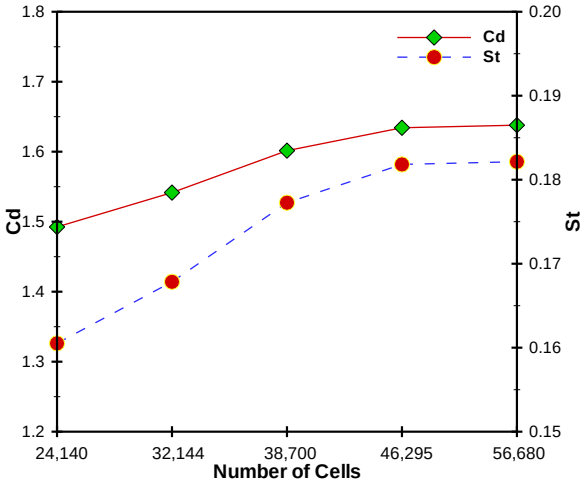

Figure 3. Mesh independency study for mean drag coefficient (left axis) and Strouhal number (right axis).

TABLE I. Verification of the Provided Results and some Experimental and Numerical Data in the Literature.

	Method	Cd	Cl	Clrms	St	Re	α	AS
Present Study	Num.	1.63	0.18	0.124	0.182	100	45	0.1
Dutta et al. [11]	Exp.	1.10	N/A	N/A	0.15	100	45	1.0
Norberg [20]	Exp.	1.65	N/A	N/A	0.17	1000	45	0.2
Sohankar and Etminan [4]	Num.	1.48	0	N/A	0.146	100	0	1.0
Sohankar et al. [16]	Num.	1.47	0	0.156	0.146	100	0	0.1
Cheng et al. [21]	Num.	1.44	0	0.152	0.144	100	0	0.1
Gera et al. [22]	Num.	1.46	0	0.157	0.129	100	0	1.0
Park and Son [23]	Num.	2.20	0	0.240	0.165	100	0	0.1

46% greater than the lift. Meanwhile, the time-averaged of total drag and lift forces are 1.63 and 0.18 respectively (see Table 1 for further details.). Interestingly, it is also realized that more than 95% of the drag and just one-third of the lift forces are belonged to the pressure component.

One complete cycle of the lift coefficient in a fully periodic flow regime is illustrated in Fig. 5 simultaneous with one cycle of drag coefficient. As it clearly seen, these forces are antiphase, with a phase lag of π (180 degrees). It means that the maximum value of the lift coefficient (the point labeled with b) happens when the drag coefficient is at the lowest value (the point labeled with b') and vice versa. On the other hand, the mean values of both coefficients (the points labeled with c and c') do not be happened at the same time. This time lag is caused by a dominant component of drag force, which is produced by the remarkable streamwise pressure gradient between the frontal and the rear sides of the bluff body.

To have a clear and deep understanding of the physics of the flow, instantaneous streamlines are colored by velocity, vorticity, and temperature at two important moments; the maximum values of lift and drag coefficients, in which are shown in Fig. 6. According to the results, the Y-velocity

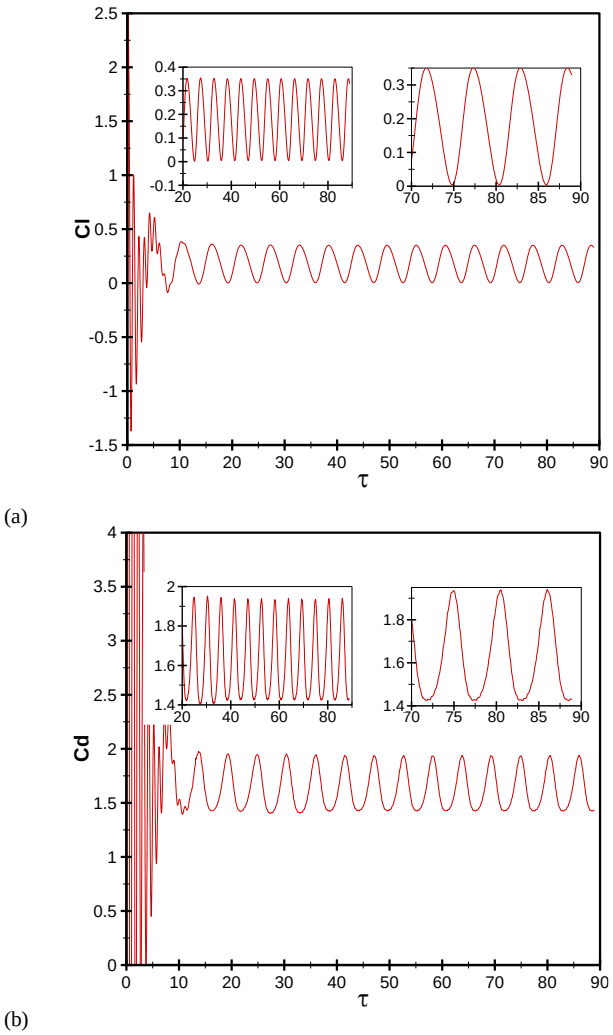

Figure 4. Time-histories of (a) lift and (b) drag coefficients (two zoomed-in views are also illustrated for more details).

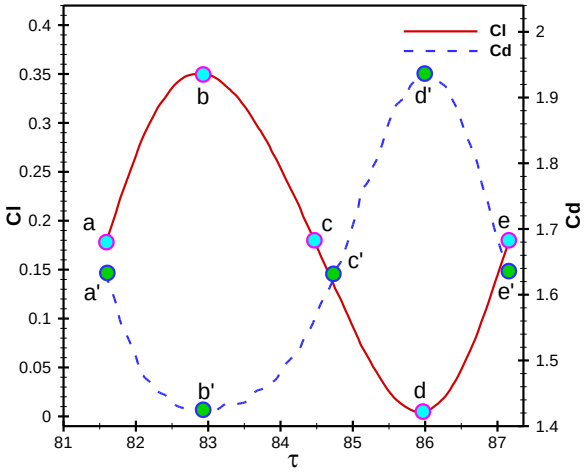

Figure 5. The one cycle time-histories of lift and drag coefficients.

difference between frontal and rear regions of the cylinder is remarkable and causes maximum lift force as well. Meanwhile, the X-velocity component is experienced the highest difference between the frontal and rear sides and makes the maximum drag coefficient accordingly. Besides, the position of the low-pressure vortex region behind the bluff body is located at the top-rear corner of the cylinder, providing the possibility of maximum lift force (centre column in Fig. 6). The developed wake (lower row in Fig. 6) causes an increase of drag force, which is the highest at the moment of maximum drag force. It is also observed that the highest and lowest temperature gradient (see the right column in Fig. 6) are happened adjacent to the frontal and rear sides of the body respectively.

The instantaneous patterns of some of the flow parameters are shown in Fig. 7. The negative X-velocity component behind the body means the movement of the wake region to the upstream, which is clearly depicted in Fig. 7. By moving away from the solid walls, flow velocity is recovered as the inlet flow. By having a look at the velocity components and vorticity contours simultaneously, it is found that the upward and downward Y-velocity in combination with the X-component push the vorticity regions towards the downstream frequently. As it seen, the highest and lowest amounts of vorticity are occurred at the bottom- and top-frontal corners of the body, where the sudden change in the geometry causes that. It should be noticed that the positive sign of the vorticity indicates the counter clockwise rotation and vice versa. Thus, the stagnation point of flow on the frontal side of the cylinder is located at the bottom one-fifth. The exact position of this point depends on the angle of incidence and inlet flow direction too.

VII. Conclusions

Numerical computation of laminar vortex shedding around a very slender vortex generator with a rectangular cross-section area is carried out for Reynolds number of 100, Prandtl number of 0.71, the aspect ratio of 0.1, and the angle of incidence of 45 degrees. It is found that after a specific time, the eddy will shed in downstream with a constant frequency. Due to the 45 degrees angle of incidence of the bluff body, more than 95% of net drag and one-third of lift forces are related to the pressure component. It is also observed that the sinusoidal drag and lift

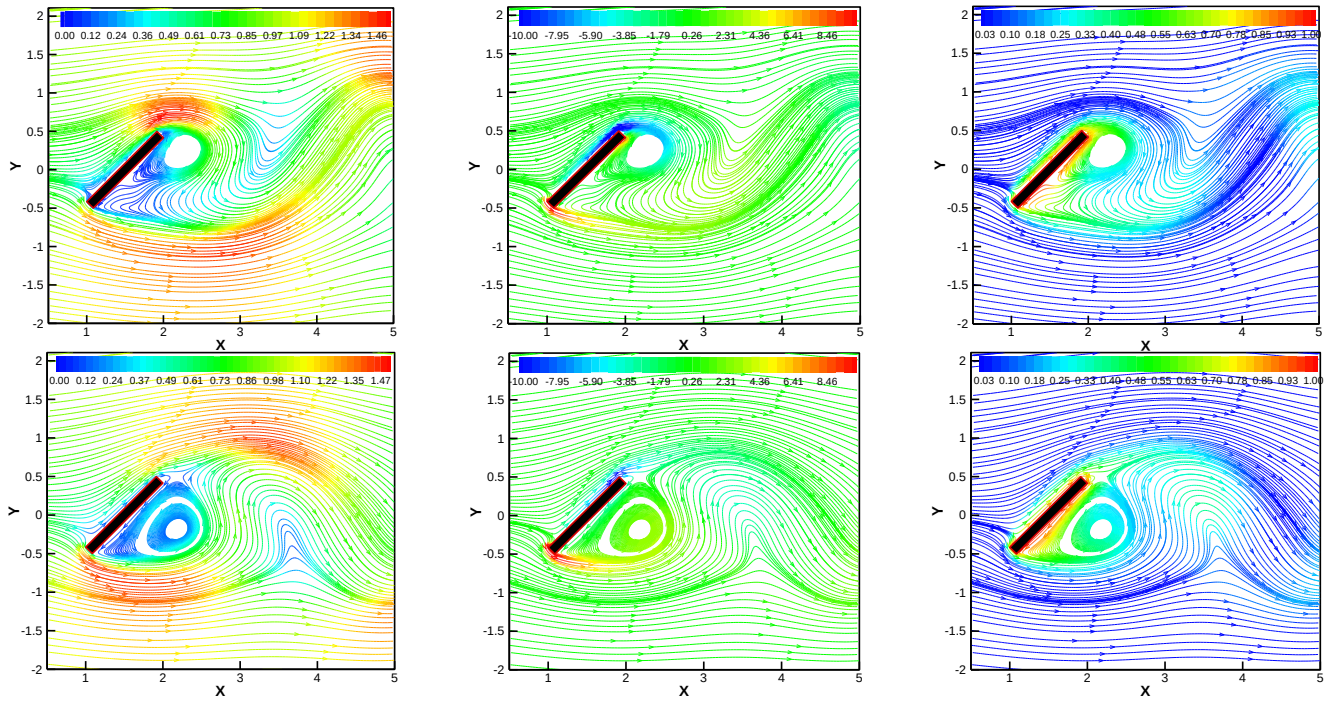

Figure 6. Instantaneous streamlines colored by velocity (left column), vorticity (centre column), and temperature (right column) at the moment of maximum lift (upper row) and maximum drag (lower row).

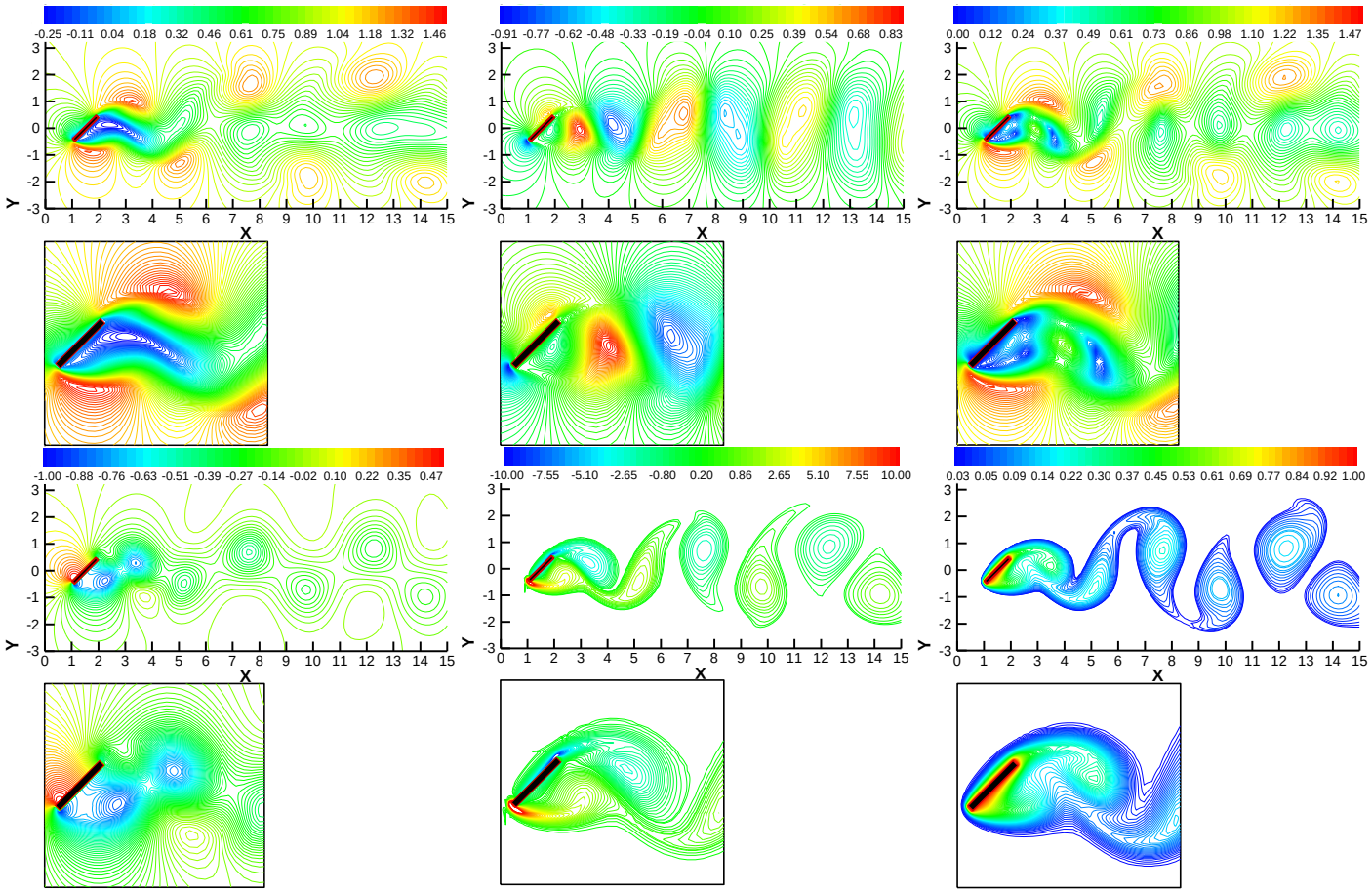

Figure 7. Instantaneous contours of X-velocity, Y-velocity, and velocity on the upper row and from left to right respectively and pressure, vorticity, and temperature on the lower row and from left to right respectively, (see the zoomed-in views under each graph for further details).

forces have 180° phase lag. This means that maximum drag force occurs simultaneously with minimum lift force and vice versa. The flow separation points are located at the leading and the trailing edges of top and bottom sides, where the maximum value of vorticity is created. Eventually, the stagnation point of flow occurs at the bottom one-fifth of the frontal side of the body, where the angle of incidence causes the movement from the centre of the frontal side toward an end.

ACKNOWLEDGMENT

The research was supported by NSERC through the Discovery Grants program.

NOMENCLATURE

English Letters

AS	aspect ratio
Cd	total drag coefficient
Cl	total lift coefficient
Clrms	root mean square of lift coefficient
d	the height of the bluff body
f	the frequency of vortex shedding
H	the dimensionless height of computational domain
k	fluid thermal conductivity coefficient
p	pressure
P	non-dimensional pressure
Pr	Prandtl number
Re	Reynolds number
St	Strouhal number
t	time
T_{in}	free stream temperature
T_w	the wall temperature of the bluff body
u	streamwise velocity component
U	dimensionless streamwise velocity component
u_{in}	free stream velocity
v	transverse velocity component
V	dimensionless transverse velocity component
x	the streamwise axis of coordinate system
X	the dimensionless streamwise axis of the coordinate system (=x/d)
Xd	dimensionless streamwise distance between the rear top corner of the bluff body and the exit plane
Xu	dimensionless streamwise distance between the inlet plane and the frontal bottom corner of the bluff body
y	the transverse axis of coordinate system
Y	the dimensionless transverse axis of coordinate system (=y/d)

Greek Letters

α	thermal diffusion coefficient
θ	dimensionless temperature
ν	fluid kinematic viscosity
ρ	fluid density
τ	dimensionless time

REFERENCES

[1] M.M. Alam, M. Moriya, K. Takai, and H. Sakamoto, "Fluctuating fluid forces acting on two circular cylinders in a tandem arrangement at a subcritical Reynolds number," Journal of Wind Engineering and Industrial Aerodynamics, vol. 91(1-2), pp. 139-154, 2003.

[2] M.M. Alam, and Y. Zhou, "Phase lag between vortex shedding from two tandem bluff bodies," Journal of Fluids and Structures, vol. 23(2), pp. 339-347, 2007.

[3] T. Kitagawa, and H. Ohta, "Numerical investigation on flow around circular cylinders in the tandem arrangement at a subcritical Reynolds number," Journal of Fluids and Structures, vol. 24(5), pp. 680-699, 2008.

[4] A. Sohankar, and A. Etminan, "Forced-convection heat transfer from tandem square cylinders in cross flow at low Reynolds numbers," International Journal for Numerical Methods in Fluids, vol. 60(7), pp. 733-751, 2009.

[5] S. Kim, M.M. Alam, H. Sakamoto, and Y. Zhou, "Flow-induced vibrations of two circular cylinders in tandem arrangement. Part1: characteristics of vibration," Journal of Wind Engineering and Industrial Aerodynamics, vol. 97(5-6), pp. 304-311, 2009.

[6] D. Sumner, "Two circular cylinders in cross-flow: A review," Journal of Fluids and Structures, vol. 26(6), pp. 849-899, 2010.

[7] L. Bruno, M.V. Salvetti, and F. Ricciardelli, "Benchmark on the aerodynamics of a rectangular 5:1 cylinder: An overview after the first four years of activity," Journal of Wind Engineering and Industrial Aerodynamics, vol. 126, pp. 87-106, 2014.

[8] M.M. Liu, L. Lu, B. Teng, M. Zhao, and G.Q. Tang, "Re-examination of laminar flow over twin circular cylinders in tandem arrangement," Fluid Dynamics Research, vol. 46(2), pp. 1-22, 2014.

[9] S. Dutta, K. Muralidhar, and P.K. Panigrahi, "Influence of the orientation of a square cylinder on the wake properties," Experiments in Fluids, vol. 34(1), pp. 16-23, 2003.

[10] B.W.V. Oudheusden, F. Scarano, N.P.V. Hinsberg, and D.W. Watt, "Phase-resolved characterization of vortex shedding in the near wake of a square-section cylinder at incidence," Experiments in Fluids, vol. 39(1), pp. 86-98, 2005.

[11] S. Dutta, P.K. Panigrahi, and K. Muralidhar, "Experimental investigation of flow past a square cylinder at an angle of incidence," Journal of Engineering Mechanics, vol. 134(9), pp. 788-803, 2008.

[12] G. Schewe, "Reynolds-number-effects in flow around a rectangular cylinder with aspect ratio 1:5," Journal of Fluids and Structures, vol. 39, pp. 15-26, 2013.

[13] C. Mannini, A.M. Marra, L. Pigolotti, and G. Bartoli, "Vortex-shedding mechanism for the BARC rectangular section in smooth and turbulent flow," 8th International Colloquium on Bluff Body Aerodynamics and Applications, Northeastern University, Boston, Massachusetts, USA, June 7-11, 2016.

[14] C. Mannini, A.M. Marra, L. Pigolotti, and G. Bartoli, "The effects of free-stream turbulence and angle of attack on the aerodynamics of a cylinder with rectangular 5:1 cross section," Journal of Wind Engineering and Industrial Aerodynamics, vol. 161, pp. 42-58, 2017.

[15] M. Ricci, L. Patruno, S. de Miranda, and F. Ubertini, "Flow field around a 5:1 rectangular cylinder using LES: Influence of inflow turbulence conditions, spanwise domain size, and their interaction," Computers and Fluids, vol. 149, pp. 181-193, 2017.

[16] A. Sohankar, C. Norberg, and L. Davidson, "Low-Reynolds-number flow around a square cylinder at incidence: a study of blockage, the onset of vortex shedding and outlet boundary condition," International Journal for Numerical Methods in Fluids, vol. 26(1), pp. 39-56, 1998.

[17] A. Etminan, M. Moosavi, and N. Ghaedsharafi, "Determination of flow configurations and fluid forces acting on two tandem square Cylinders in cross-flow and its wake patterns," International Journal of Mechanics, vol. 5(2), pp. 63-74, 2011.

[18] A. Etminan, and A. Barzegar, "Instantaneous and time-averaged flow structure around two heated square cylinders in the laminar flow Regime," Applied Mechanics and Materials Journal, vol. 110-116, pp. 2898-2902, 2012.

[19] A. Etminan, "Flow and heat transfer over two bluff bodies from very low to high Reynolds numbers in the laminar and turbulent flow regimes," International Journal of Advanced Design and Manufacturing Technology, vol. 6(2), pp. 61-72, 2013.

[20] C. Norberg, "An Experimental investigation of the flow around a circular clinder: in fluence of aspect ratio," Journal of Fluid Mechanics, vol. 258, pp. 287-316, 1993.

[21] M. Cheng, D.S. Whyte, and J. Lou, "Numerical simulation of flow around a square cylinder in uniform-shear flow," Journal of Fluids and Structures, vol. 23(2), pp. 207-226, 2007.

[22] B. Gera, P.K. Sharma, and R.K. Singh, "CFD analysis of 2D unsteady flow around a square cylinder," International Journal of Applied Engineering Research, vol. 1(3), pp. 602-610, 2010.

[23] Y.G. Park, and C.M. Son, "A numerical study on flow characteristics around rectangular cylinder with different width-to-height ratios," Korean Journal of Air-Conditions and Refrigeration Engineering, vol. 22(8), pp. 523-529, 2010.